A Channel Model for land mobile satellite navigation

Alexander Steingass
*Institute of Communications and Navigation
German Aerospace Center (DLR)
Muenchnerstrasse 20
D-82234 Wessling, Germany
Tel: +49 8153 28-2864
Email: alexander.steingass@dlr.de

Andreas Lehner
Institute of Communications and Navigation
German Aerospace Center (DLR)
Muenchnerstrasse 20
D-82234 Wessling, Germany
Tel.: +49 8153 28-2804
Email: andreas.lehner@dlr.de

August 8, 2005

Abstract

In 2002 the German Aerospace Centre (DLR) performed a measurement campaign of the land mobile multipath channel. From this data we derived a channel model that is synthesising the measured channel impulse response. It allows the realistic simulation of the multipath channel by approximating every single reflection. This model includes time variant reflectors approaching and receding, appearing and disappearing reflectors and a variation of the azimuth and elevation of the satellite. All the signal processing had been realised independently of the transmitted signal. Therefore the usability for both navigation systems (GPS as well as GALILEO) or other wide band systems is given.

*Corresponding author.

1 Introduction

Beside the ionosphere one of the most significant problems to achieve an accurate navigation solution for both GPS and GALILEO within cities is the multipath reception. Various channel models do exist for ground to ground communications (e.g. COST 207 for the GSM system). But there is still a lack of knowledge for broadband satellite to earth channels [1]. Therefore the German Aerospace Centre (DLR) performed a measurement campaign in 2002. In this campaign we used a Zeppelin to simulate a satellite transmitting a 100 MHz broadband signal towards earth. To ensure a realistic scenario the signal was transmitted between 1460 and 1560 MHz just nearby the GPS L1 band. This signal was received by a measurement van and was recorded using a regular time grid. The so gathered data was then passed through a super resolution algorithm to detect the single reflections. In a further step we tracked the detected reflections in time and gained a knowledge about the characteristics of any isolated reflection. This includes both Doppler shift and delay of the reflection. On top of this we gained knowledge about the direct path behaviour.

2 Direct Path

In an open environment the direct path would be best represented by the line of sight (LOS) transmission of the signal. In the following we name all measurements relatively to this LOS path. In an urban environment this LOS is blocked so that the signal is attenuated and possibly delayed with respect to the LOS. As obstacles we had been able to identify three major obstacles in cities that influences the signal reception.

1. House fronts
2. Trees
3. Light posts

2.1 The influence of House fronts

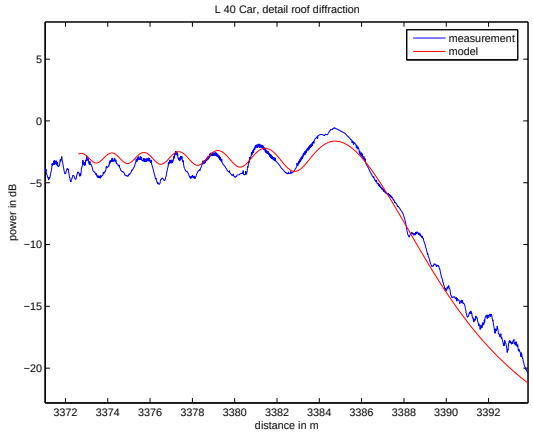

Figure 1: Diffraction by a house front measurement in comparison to the model used

When the LOS ray hits the house front obviously the signal is affected. Figure 1 shows the vehicle on a track during the measurement driving into the shadow of the building. The x-axis indicates the driven distance from start. At about 3885 m from the vehicle is entering the shadowing area. From this instance the signal is strongly attenuated. This behaviour is well known from the so called "Knife Edge Model" [2]. In this model it is assumed that a planar wave is hitting a half sided infinitively large plate. The calculated attenuation from this model is also displayed in Figure 1. From this comparison the concurrence of measurement and model is obvious. Therefore the knife edge model is selected to model this effect. This process is motion dependent only.

2.2 The influence of trees

As it is shown in figure 2 the LOS signal is attenuated by trees. The measured process on the one hand side is dependent on the length of the LOS signal being within the tree, on the other hand side an additional process is visible caused by branches or leafs attenuating. In contrast to approaches where branches are modelled by ray tracing models [3] we use a combination of an attenuating only cylinder modelling the transmission trough the tree and a statistical fading process modelling the branches. This process is motion dependent only.

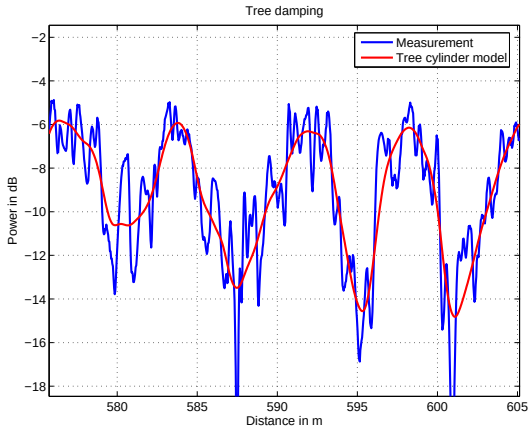

Figure 2: Signal attenuation by series of trees - comparison of measurement and model

2.3 The influence of lightposts

Surprisingly a lightpost has a strong influence to the LOS signal. Figure 3 shows an example of a 20 cm lamppost. When passing by such a post the strength of the signal begins to oscillate goes down quickly in the direct shadow of the post and comes

up again oscillating behind. We model a lamppost with a "double knife edge model" where we assume to overlapping knife edges being present. One is reaching from $-D/2 < x < \infty$ and the other is reaching from $-\infty < x < D/2$. Both edges are simulated separately and then added coherently. Figure 3 shows the near perfect match of model and measurement. This process is also motion dependent only.

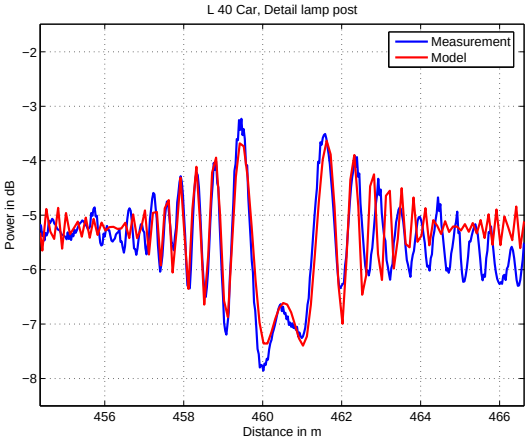

Figure 3: LOS signal being affected by a lightpost - comparison of measurement and model

3 Reflected Signal

In the measurement data reflections appear often [4, 5]. In contrast to ray tracing algorithms [6] we do not model a specific scenery. We assume reflections to be statistically distributed in the x,y,z space and generate them statistically. In order to match the measured statistic we must take a closer look to the echo distribution.

3.1 Influence of the relative angle

Lets assume a receiver to be at position RX, a satellite at position S and a reflector at position R. Then the relative receiving angle α is the angle at the receiver (see figure 4). We can see a clear dependency of the relative angle in the measurement data (see figure 5). For this figure we

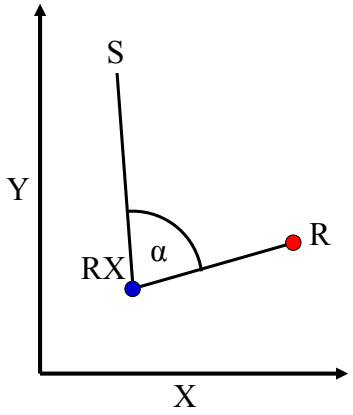

Figure 4: Definition of the relative angle α.

averaged over all occurring absolute azimuth angles by

$$\bar{p}(\alpha) = \frac{\sum p(\alpha)}{\sum \alpha} \tag{1}$$

taking into account the likelihood of the relative angle α to occur. This on the first look astonishing result can be easily understand if one has in mind the very rectangular structure of urban cities. Due to this structure a corner reflector (see figure 6) occurs very often in cities. The main characteristic of this reflector is that a ray coming from a satellite is being reflected back into the satellite direction in the x-y plane. Its elevation is unchanged. Then it is obvious that it is most likely to receive reflections from the opposite side of the satellite.

3.2 Geometric occurrence of reflectors

Figure 7 shows the likelihood distribution of reflectors. In this figure the receiver is moving in x-direction only. It can clearly be seen that the highest likelihood of receiving a reflector is when the reflector is on the right or on the left side. The likelihood of receiving a reflector from the front is close to zero. This as well on the first look astonishing result becomes more plausible when on has in mind an urban canyon. It must be unlikely that a reflecting obstacle is in near front position of the car, otherwise one would overrun it in the next

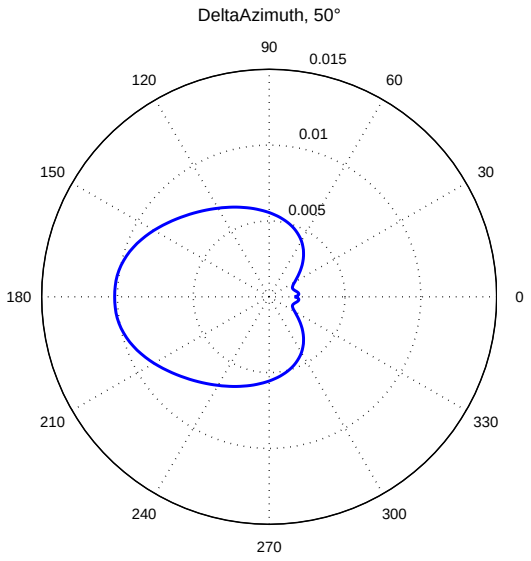

Figure 5: Likelihood distribution of the relative angle.

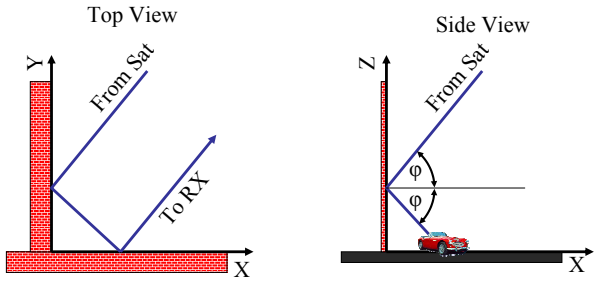

Figure 6: Corner reflectors as it can be often found in cities.

second. To calculate the conditional likelihood of a reflector being present at a certain position one has to multiply the statistic shown in figure 5 and 7. The result of this operation is shown in figure 8, here the satellites position had been chosen at 25° azimuth.

3.3 Lifespan of reflectors

In the measurement data the channel appears rapidly changing. Many echoes disappear and others appear at new positions. This process is highly correlated to the receiver speed. When the car stops the reflections remain in the scenery. Therefore we defined a life distance of each reflector. This life distance is the distance the receiver is travelling until the echo disappears. Figure 9 shows a histogram of the echo life distance. It can be seen that the life distance of the reflectors is usually well below 1 m. Most Reflectors exist along a motion path below 5 m. Therefore the channel is changing rapidly.

3.4 Mean power of reflectors

Figure 10 shows the power distribution in dependency of the relative position. Since reflectors in the real world have a given geometrical size of course their distance plays a major role for the mean power. Having again in mind the urban canyon it is quite understandable that the most powerful reflections are on the sides of the streets. With increasing distance the mean power of the reflections is decreasing. Beside the mean power map we have derived a power variance map (not shown) to allow the process a certain variation.

3.5 Fading process of reflections

When the receiver is moving it drives through a quasi stationary field radiated by the reflectors. Therefore the receiver recognises a variation of the actual power of the reflector (see also figure 12). Interesting enough this fading process does not even come to a stop when the car does not move. We assume that the channel is changing for example due to trees in the wind, other cars... Furthermore there was no correlation between this fading process and the receiver speed. Therefore we assume this process to be time dependent only. The typical bandwidth of such a process is in the range of some Hertz. The deepness of the fades is expressed by the Rice factor K_{Rice}.

$$K_{Rice} = \frac{P_{Constant}}{P_{fading}} \tag{2}$$

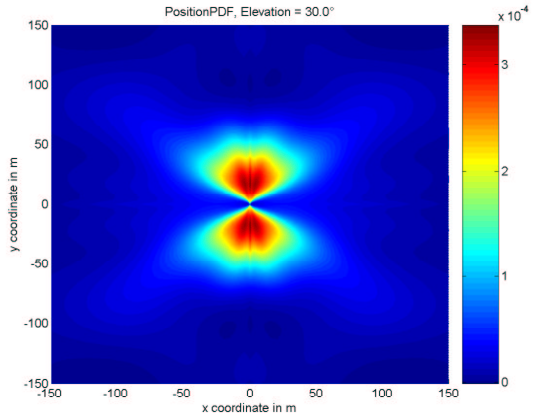

Figure 7: Likelihood of reflectors being at a certain position. Moving direction of the receiver is in x-Direction only.

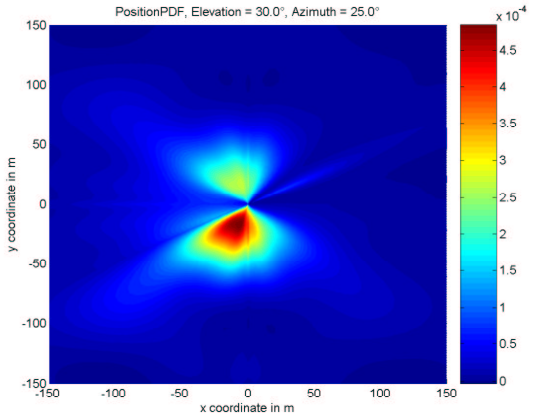

Figure 8: Conditional likelihood of reflectors being at a certain position. Satellite at 25° azimuth.

It defines the ratio between the constant power $P_{Constant}$ and the power of the fading process P_{fading}. Figure 11 shows the distribution of the Rice factor.

3.6 Time series characteristic of reflectors

Classical channel models like the GSM channel model [7] use time invariant path delays and model the change of the reflector over the time by the assumption that many echoes are received at around the same path delay and their absolute azimuth is equally distributed. The resulting Doppler spectrum, the so called Jakes spectrum [8], is given by:

$$bP(f_D) = \begin{cases} \frac{\text{const}}{\sqrt{1-\left(\frac{f_D}{f_{Dmax}}\right)^2}} & \forall\, |f_D| < f_{Dmax} \\ 0 & \text{else,} \end{cases} \quad (3)$$

This approach is feasible for narrow band systems like GSM but in a wide band system such as GPS/GALILEO we regard the modelling accuracy as insufficient.

Figure 12 shows the sliding window Fourier transform of an isolated reflection. There it can be seen that the echo is best characterised by a trace in Doppler frequency. Within 1.6 s the Doppler frequency of the reflector changes from +30 Hz to -5 Hz. In the same period the path delay of the reflector changes. The variability of the reflector is clearly dependent of the vehicle speed. Therefore we realise the channel model as a geometrical representation. This means that we initialise a reflector at a randomly chosen position (according to the measured statistics) and pass by with a receiver with the actual speed. Then both path delay and phase of the reflection can be calculated geometrically. This causes the main process to be motion dependent only. Figure 13 shows how a single reflector is modelled. In terms of the reflector the artificial scenery generates a continues series of receiver position according to the actual speed. The receiver is moving only in x-direction. To simulate turns the relative azimuth of the satellite is changed.

3.7 Number of echoes

During a drive through a city the number of echoes being received changes. For a navigation receiver that tries to estimate the channel impulse response (super resolution for multipath mitigation) a high number of reflections is a "high stress scenario". Other phases with a lower number of echoes are less critical for it. Beside the mean number of

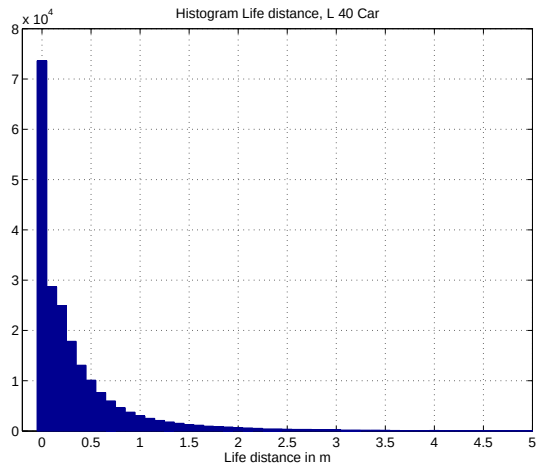

Figure 9: Live distance of echoes.

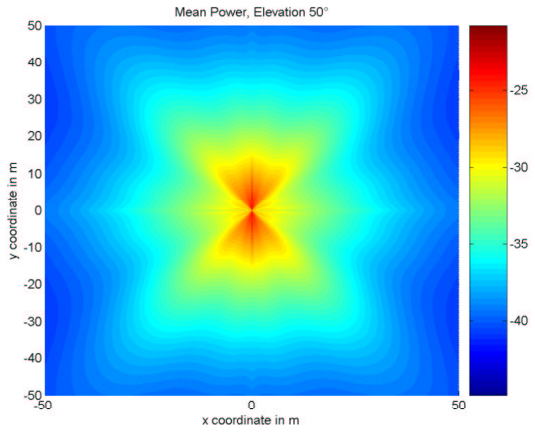

Figure 10: Mean power of the reflectors in dependency of their relative position.

echoes therefore it is very important to model exactly this increasing and decreasing process. A sample of it is shown in figure 14. Please note the relatively high number of echoes (up to 50) at the same time. We had been able to detect two processes: An extremely narrow band process with high power and a lower powered wide band process. Their combination results in a very good approximation of the process.

4 Examples

In figure 17 - 20 an example output of the channel model is given. In this scenario the car drove with a variable speed through the city. The speed was a $\sin(t)$ like function. At 4.71 s the speed of the vehicle was nearly 0 km/h. In figure 18 the doppler shift of every echo is shown. The red dotted line is the theoretical limit for the Doppler shift given by

$$f_{Doppler} = \frac{\vec{v} \cdot (\vec{Rx} - \vec{Sat}) \cdot f_c}{C_0} \tag{4}$$

where $\vec{v}$ is the speed vector of the vehicle, $\vec{Rx}$ is the receiver position, f_c is the carrier frequency, $\vec{Sat}$ is the satellite Position and C_0 is the speed of light. In this figure or in the Extract (figure 20) one can determine isolated echoes changing their Doppler shift during their life distance (for example the mint green colored echo lasting from 0.82 - 1.35 s. The rapid changes in the channel are visible within the displayed period of around one second many echoes die and others are generated. Around the standstill the channel does not change much - clearly visible by the low Doppler bandwidth and the long lasting echoes (long lines) in figure 17. In this situation only the time driven fading process is changing the channel. But neither an echo is terminated nor a new one is generated in this situation. Furthermore one can see regions where more echoes are present than in others. Due to this precise modelling of reflections new receiver algorithms can be tested very well.

5 Summary

In this paper we have shown our new channel model for the land mobile multipath channel. This channel model is based on a new approach: The combination of statistical data from a measurement and a deterministic scenario. The deterministic scenario is used for the direct path modelling. This includes effects such as shadowing by house fronts, tree damping or refracting lightposts. The reflections of this channel model are generated statistically in the geometric scenario. Their generation is driven by data obtained from the measure-

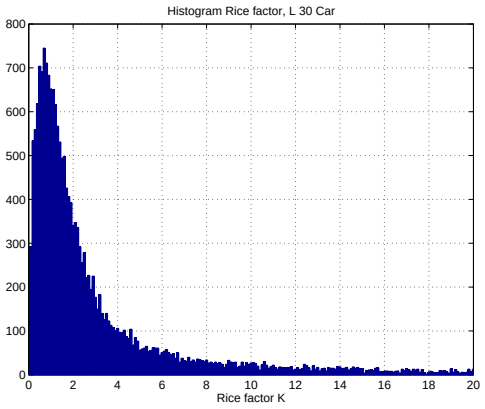

Figure 11: Rice factor histogram of the fading process.

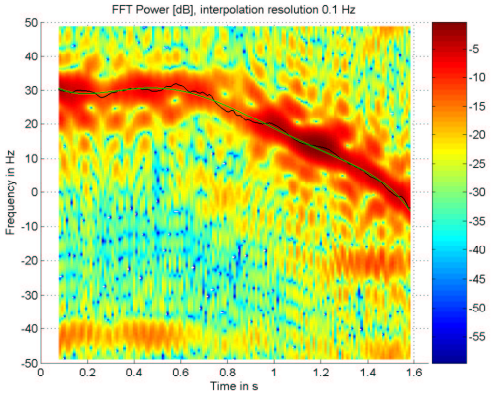

Figure 12: Sliding window Fourier transform of an isolated reflection.

ment only. The model includes:

- Elevation changes,
- azimuth changes,
- speed changes
- and a variable number of reflectors.

The model will be available for download soon: http://www.kn-s.dlr.de/satnav/

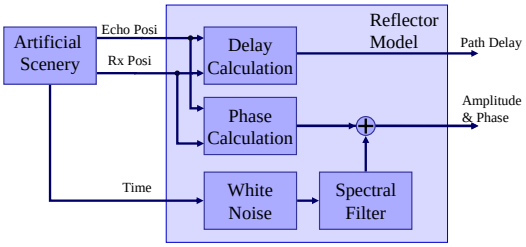

Figure 13: Model of an isolated reflector

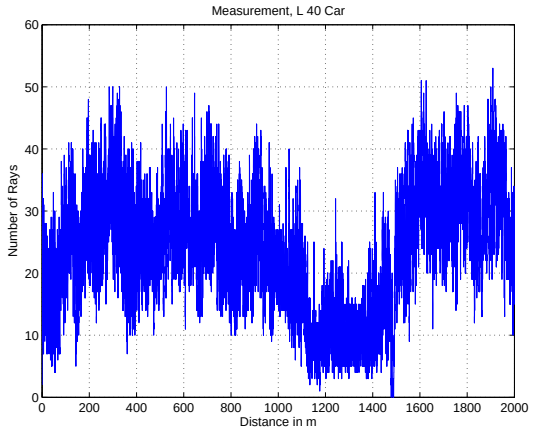

Figure 14: Number of echoes at the same time during a 15 min drive trough a city.

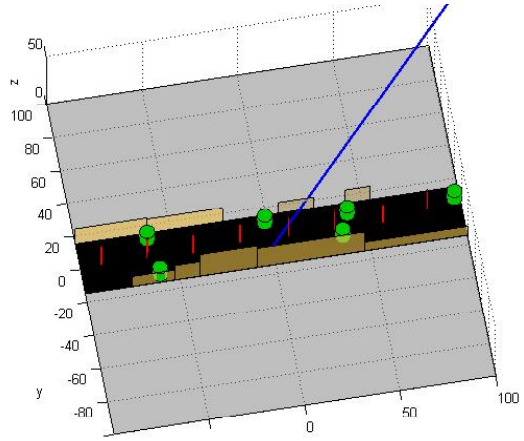

Figure 16: A picture of the artificial scenery. Brown are house fronts, green cylinders are trees, red are poles.

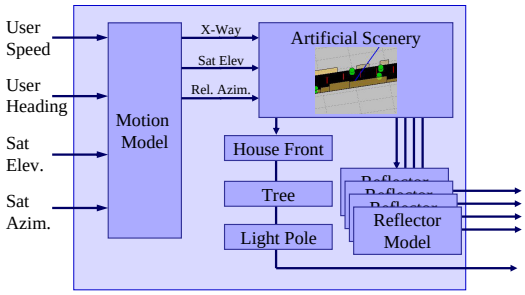

Figure 15: Block diagram of the channel model.

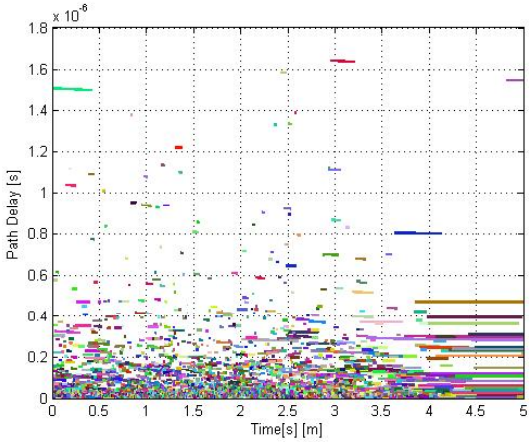

Figure 17: Example of generated echoes. Plotted is the path delay of the reflections over time.

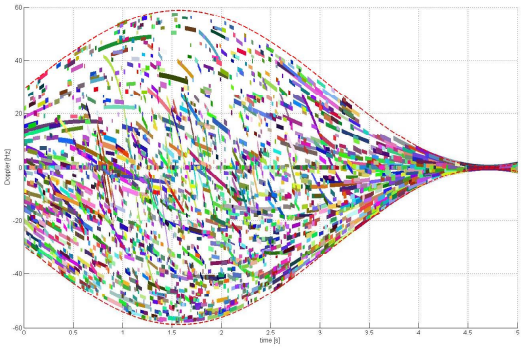

Figure 18: Example of generated echoes. Plotted is the Doppler of the reflections over time.

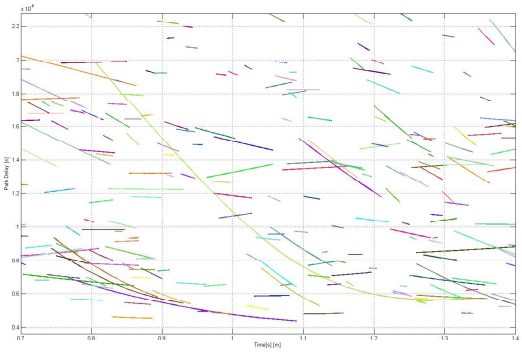

Figure 19: Extract of figure 17.

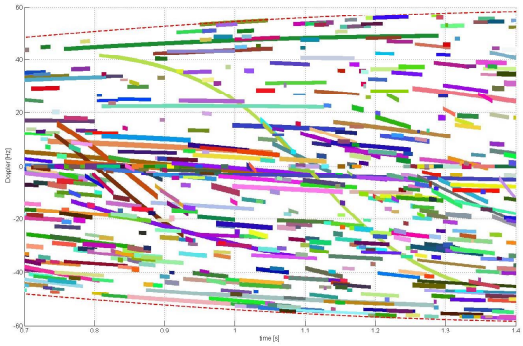

Figure 20: Extract of figure 18.

References

[1] R. Schweikert, T. Woerz. Signal design and transmission performance study for GNSS-2. Technical note on digital channel model for data transmission, European Space Agency, 1998.

[2] J. S. Orfanidis. *Electromagnetic Waves and Antennas*. Online www.ece.rutgers.edu/ orfanidi/ewa, Rutgers University, June 2004.

[3] Yvo L. C. de Jong and Matti H. A. J. Herben. A tree-scattering model for improved propagation prediction in urban microcells. *IEEE Transactions on Vehicular Technology*, pages 503–513, March. 2004.

[4] Alexander Steingass, Andreas Lehner. Measuring the navigation multipath channel a statistical analysis. *ION GPS 2004 Conference Long Beach, California USA*, September 2004.

[5] Alexander Steingass, Andreas Lehner. Measuring galileos multipath channel. *Global Navigation Satellite Systems Conference (GNSS2003), Graz, Austria*, 2003.

[6] O. Esbri-Rodriguez, A. Konovaltsev, und A. Hornbostel. Modeling of the gnss directional radio channel in urban areas based on synthetic environments. *Proceedings of ION NTM*, Jan. 2004.

[7] COST 207 WG1. Proposal on channel transfer functions to be used in GSM tests 1986. Technical report, CEPT Paris, 1986.

[8] W.C. Jakes. *Microwave Mobile Communications*. John Wiley & Sons, Inc. , New York, 1974.

[9] B.W. Parkinson, J.J. Spilker. *Global Positioning System Theory and Applications I*, volume 163 of *Progress in Astronautics and Aeronautics*. American Institute of Aeronautics and Astronautics, Inc, Washington, 1996.

[10] B.W. Parkinson, J.J. Spilker. *Global Positioning System Theory and Applications II*, volume 164 of *Progress in Astronautics and Aeronautics*. American Institute of Aeronautics and Astronautics, Inc. , Washington, 1996.